



UNIVERSITY OF LEEDS

This is a repository copy of *Chloride binding and diffusion in slag blends: Influence of slag composition and temperature*.

White Rose Research Online URL for this paper:
<http://eprints.whiterose.ac.uk/117228/>

Version: Accepted Version

Article:

Ogirigbo, OR and Black, L orcid.org/0000-0001-8531-4989 (2017) Chloride binding and diffusion in slag blends: Influence of slag composition and temperature. *Construction and Building Materials*, 149. pp. 816-825. ISSN 0950-0618

<https://doi.org/10.1016/j.conbuildmat.2017.05.184>

© 2017 Elsevier Ltd. Licensed under the Creative Commons Attribution-NonCommercial-NoDerivatives 4.0 International
<http://creativecommons.org/licenses/by-nc-nd/4.0/>

Reuse

Items deposited in White Rose Research Online are protected by copyright, with all rights reserved unless indicated otherwise. They may be downloaded and/or printed for private study, or other acts as permitted by national copyright laws. The publisher or other rights holders may allow further reproduction and re-use of the full text version. This is indicated by the licence information on the White Rose Research Online record for the item.

Takedown

If you consider content in White Rose Research Online to be in breach of UK law, please notify us by emailing eprints@whiterose.ac.uk including the URL of the record and the reason for the withdrawal request.



eprints@whiterose.ac.uk
<https://eprints.whiterose.ac.uk/>

1 **Chloride binding and diffusion in slag blends: influence of slag composition**
2 **and temperature**

3 **Okiemute Roland Ogirigbo^{a,b*}, Leon Black^b**

4 ^aDepartment of Civil Engineering, Faculty of Engineering, University of Benin,
5 Ugbowo, Benin City, Nigeria

6 ^bInstitute of Resilient Infrastructure, School of Civil Engineering, University of Leeds,
7 Woodhouse Lane, Leeds LS2 9JT, United Kingdom

8 ^{a,b*}okiemute.ogirigbo@uniben.edu, ^bL.Black@leeds.ac.uk

9 *Corresponding author. Tel: +234 (0) 813 696 2171, Email address:

10 okiemute.ogirigbo@uniben.edu

11 **Abstract**

12 This study has investigated the impact of a change in GGBS chemical composition
13 on the chloride ingress resistance of slag blended cements under different
14 temperature regimes. Two slags, having alumina contents of 12.23 and 7.77%
15 respectively, were combined with a CEM I 52.5 R at 30 wt% replacement. Chloride
16 binding and diffusion tests were conducted on paste and mortar samples
17 respectively. All tests were carried out at temperatures of 20°C and 38°C. The higher
18 temperature resulted in an increase in chloride binding; attributed to greater degrees
19 of slag hydration. Despite this, chloride ingress was greater at 38°C; attributed to
20 changes in the pore structure and the chloride binding capacities of the slag blends.
21 The more reactive, aluminium-rich slag performed better in terms of chloride binding
22 and resistance to chloride penetration, especially at the high temperature and this
23 was attributed to its higher alumina content and greater degree of reaction at 38°C.

24 **Keywords:** Chloride binding, Granulated Blast-Furnace Slag, Temperature, Diffusion,
25 **Microstructure**

26 1. Introduction

27 Chloride-induced corrosion of steel reinforcement is one of the major causes of
28 premature deterioration and degradation of concrete structures built in marine
29 environments. Chlorides may be introduced into concrete through a variety of routes,
30 for example as de-icing salts, through the penetration of seawater, through the use
31 of aggregates contaminated with chlorides or through the mix water [1]. The
32 presence of chlorides in concrete may cause disruption to the passive film on the
33 surface of steel reinforcement, thereby accelerating corrosion.

34 Chlorides in concrete exist either as free ions dissolved in the pore water, or bound.
35 The bound chlorides are either chemically bound with the tricalcium aluminate (C_3A)
36 phase in the form of Friedel's salt ($3CaO \cdot Al_2O_3 \cdot CaCl_2 \cdot 10H_2O$) and Kuzel's salt
37 ($3CaO \cdot Al_2O_3 \cdot 1/2CaCl_2 \cdot 1/2CaSO_4 \cdot \sim 11H_2O$) or physically bound to the surface of the
38 hydration products (C-S-H gel). It is the free chlorides present in the pore water that
39 are responsible for steel depassivation, so when more chlorides are bound, less free
40 chlorides will be available for depassivation. Several factors have been reported to
41 affect the formation of bound chlorides, such as the quantity of C_3A in the cement,
42 the incorporation of supplementary cementitious materials (SCMs) in the mix, the
43 alkalinity of the pore solution, the cation type of the salt, and the presence of other
44 anions, like sulphates and carbonates [2–9].

45 The use of ground granulated blast furnace slag (GGBS), a common SCM, to
46 partially replace Portland cement in the making of concrete has been shown to be
47 beneficial in terms of chloride binding and resistance to the penetration of chloride
48 ions [3,10–13]. This has been reflected in standards, e.g. EN197-1, where CEM
49 IIA/B-S and CEM III A/B/C cements are commonly used for marine construction.
50 The improved chloride resistance of slag composite cements has been attributed to

51 their high alumina content [3,10–12], which increases the tendency for Friedel's salt
52 formation. Furthermore, slag composite cements also contain more C-S-H phase,
53 which is responsible for the binding of about two-thirds of the chloride [14].
54 Generally, the higher the level of slag replacement, the higher the chloride binding
55 capacity [3]. A recent study by Otieno et al. [13] showed that particle fineness, as
56 well as difference in chemical composition of slags, had an impact on their chloride
57 ingress resistance. However, amongst the three types of slags they studied, only one
58 of them was GGBS. The other two were by-products of the Corex process and FeMn
59 arc-furnace slag.

60 In practice, while the chemical composition of GGBS from a single plant may be
61 constant, due to the varying sources from which GGBS is obtained the chemical
62 composition from plant to plant may vary. The chemical composition has often been
63 used as an indicator of the slag's reactivity. Oxide/basicity ratios have been
64 prescribed by several authors [15–17] for assessing the reactivity of slags. These are
65 usually based on the CaO, Al₂O₃, MgO and SiO₂ contents. While it is known that the
66 chemical composition of a slag is important as it may affect its performance, the
67 relationship between composition and performance is not clear-cut. Several
68 researchers have investigated the impact of variation of chemical composition of
69 GGBS on its performance, but most of these studies have been focused on the
70 strength performance [16–19].

71 Apart from the chemical composition, other factors such as the glass content,
72 particle fineness, alkalinity of the reacting system and temperature, have also been
73 reported to affect the reactivity of slags [20]. For example, in a recent work by the
74 authors [21] it was shown that temperature had more influence on the reactivity of
75 slags than the difference in chemical composition. Due to the variability in the use of

76 GGBS as an SCM in different temperature environments, like the tropical and
77 temperate regions, it is important to look at how temperature affects the performance
78 of slag blended cements in chloride environments. This paper focuses on the impact
79 of a difference in slag composition on the chloride binding and diffusion in slag
80 blended cements, relating it to the microstructure, and how the whole process is
81 affected by changes in both curing and testing temperature.

82 **2. Materials and methods**

83 2.1 Materials

84 Two slags (S1 and S2) were selected for this study, alongside a CEM I 52.5 R,
85 designated as C52.5R. Both slags met the requirement as specified in EN 197-
86 1:2011 [22]. They had similar physical properties and particle morphologies, but
87 different chemical compositions. The $\text{CaO}+\text{MgO}/\text{SiO}_2$ of slag 1 (1.28) was higher
88 than that of slag 2 (1.18). The oxide and phase composition of the as-received
89 cementitious materials are shown in Table 1. The particle size distribution of the
90 slags and the X-ray diffraction patterns are shown in Fig. 1 and Fig. 2 respectively.
91 Other physical properties of the cementitious materials are shown in Table 2. The
92 fine aggregate used complied with the specification for fine aggregates as given in
93 EN 12620:2002+A1.

Table 1: Oxide and phase composition of the cementitious materials

	Oxide composition (%)				Phase composition (%)		
	C52.5 R	S1	S2		C52.5R	S1	S2
LOI	2.54	(+1.66)	(+0.40)	Alite, C ₃ S	62.1		
950°C			*				
SiO ₂	19.10	36.58	40.14	Belite, C ₂ S	8.9		
Al ₂ O ₃	5.35	12.23	7.77	C ₃ A	9.1		
TiO ₂	0.25	0.83	0.30	Ferrite, C ₄ AF	8.5		
MnO	0.03	0.64	0.64	Calcite	1.8	0.3	0.5
Fe ₂ O ₃	2.95	0.48	0.78	Anhydrite	0.6		
CaO	62.38	38.24	37.90	Hemihydrate	2.4		
MgO	2.37	8.55	9.51	Gypsum	1.7		
K ₂ O	1.05	0.65	0.55	Others	5.0		
Na ₂ O	0.05	0.27	0.36	Merwinite		<0.1	2.3
SO ₃	3.34	1.00	1.47	Akermanite		0.2	<0.1
P ₂ O ₅	0.10	0.06	0.02	Illite		0.2	<0.1
Total	99.50	99.88	99.43	Total crystalline phases	100.1	0.7	2.9
Na ₂ O	0.74			Glass content		99.3	97.1

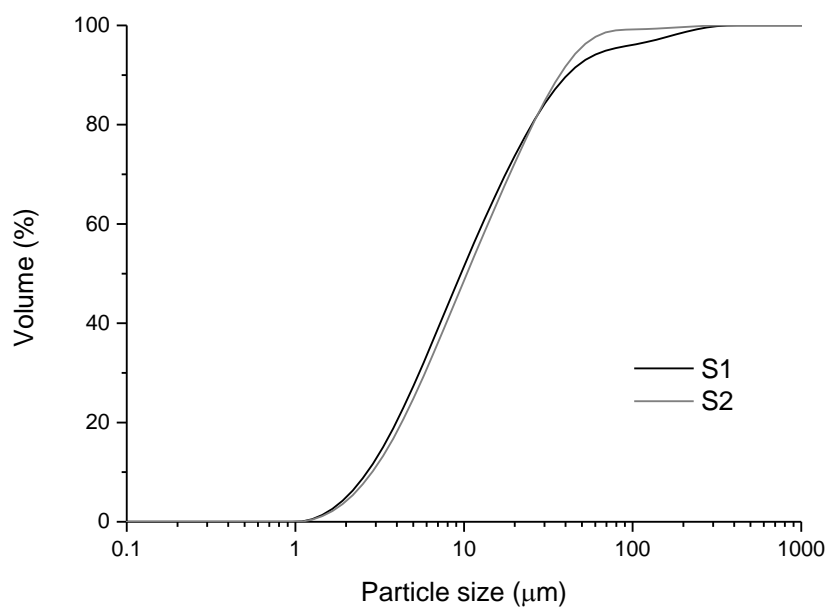
equiv.

*The sample was oxidized with HNO₃ before the determination of LOI

96 **Table 2:** Physical properties of cementitious materials

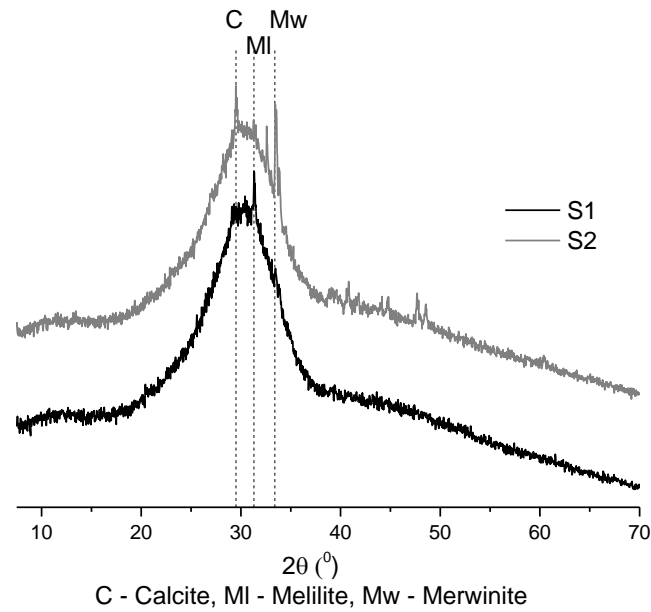
Property	Unit	C52.5R	S1	S2
Density	g/cm ³	3.18	2.94	2.95
Blaine	cm ² /g	5710	4490	4090
Particle size, d50	μm	-	11.0	11.9
Workability from flow table test	mm	-	13.13	13.55

97



98

99 **Fig. 1.** Particle size distribution of slag 1 and slag 2



100

101 **Fig. 2.** XRD of the anhydrous slags

102 2.2 Details of mixes, curing and exposure conditions

103 Two series of mixes were used for this study, with each slag being combined with a
 104 CEM I 52.5 R at 30% replacement level to produce blends designated as CS1 and
 105 CS2 respectively. The blends were prepared by mixing the various portions of the
 106 slag and cement in a laboratory ball mill for a period of about 4 hours, using
 107 polythene balls as charges.

108 Mortar samples were prepared and cured in accordance with EN 196-1:2005 [23].

109 The details of the mixes are shown in Table 3. Mixing was done in batches using a
 110 Hobart mixer. Each batch contained approximately 450 grams of cementitious
 111 materials, 1350 grams of fine aggregates and 225 grams of water. After mixing, the
 112 mortar samples were poured into moulds of 40 x 40 x 160 mm prisms or 50 mm
 113 cubes, covered with thin polythene sheets and left to cure under ambient laboratory
 114 conditions for a period of 20 – 24 hours. After the initial curing, the samples were de-
 115 moulded and cured under water at two different temperatures (20°C and 38°C) for a
 116 period up to 28 days. 20°C was chosen as a reference temperature, which is typical

117 of laboratory conditions, while 38°C was chosen as a representative temperature for
118 tropical, arid or semi-arid zones.

119 **Table 3:** Mix ratios for the mortar specimens

Mix	w/b	C52.5R	S1	S2	Water	Fines
1	0.5	0.7	0.3	0	0.5	3
2	0.5	0.7	0	0.3	0.5	3

120

121 Cement paste samples were prepared by manual mixing of the cementitious
122 materials and water by hand for 2 mins. After mixing, the resulting paste was poured
123 into 14 or 25 mm ϕ cylindrical plastic vials. The top of the plastic vials were sealed
124 with polythene and allowed to rotate vertically at 20 rpm for 24 hours so as to
125 prevent bleeding. After 24 hours, the samples were demoulded and cured in
126 saturated lime water at temperatures of 20°C or 38°C.

127 After curing, the mortar samples used for the chloride ingress studies were
128 submerged in 3% NaCl solutions kept at temperatures of 20°C or 38°C, for up to 90
129 days. For the samples exposed at 20°C, the solutions were renewed every 4 weeks
130 to maintain the salinity of the solution, and the liquid to solid ratio was kept above
131 12.5 millilitres per square centimetre of exposed surface as specified in EN
132 12390:2015 [24]. For the samples exposed to the sodium chloride solution at 38°C,
133 the solutions were renewed every fortnight so as to minimise the effect of
134 evaporation on the salinity of the solutions.

135 2.3 Test methods

136 2.3.1 Chloride binding

137 Paste samples that had been cured for 8 weeks were wet-crushed and water-sieved
138 to obtain particles ranging in size from 250 to 630 microns. The samples were dried

139 under a moderate vacuum (0.75 bar) in a desiccator at room temperature for a
140 period of 3 days to remove most of the water, then stored in a desiccator with
141 decarbonized air at 11%RH kept by saturated LiCl solution for 14 days.

142 Bound chloride content was measured using the equilibrium method, as developed
143 by Luping and Nilsson [25]. 20g of the sample dried at 11%RH was put in a plastic
144 cup and filled with approximately 50 ml of a given concentration of NaCl solution
145 saturated with Ca(OH)₂. The cup was sealed and stored at temperatures of either 20
146 or 38°C for a period of 6 weeks, to attain equilibrium. After equilibrium was reached,
147 the chloride concentration of the resulting solution was determined by ion
148 chromatography. Knowing the initial concentration of the NaCl solution, the content
149 of bound chlorides was determined using the expression:

$$150 \quad C_b = \frac{35.45V(C_i - C_f)}{W} \quad (1)$$

151 where:

152 C_b bound chloride content in mg/g-sample

153 V volume of solution in ml

154 C_i initial concentration of the chloride solution in mol/l

155 C_f equilibrium concentration of the chloride solution in mol/l

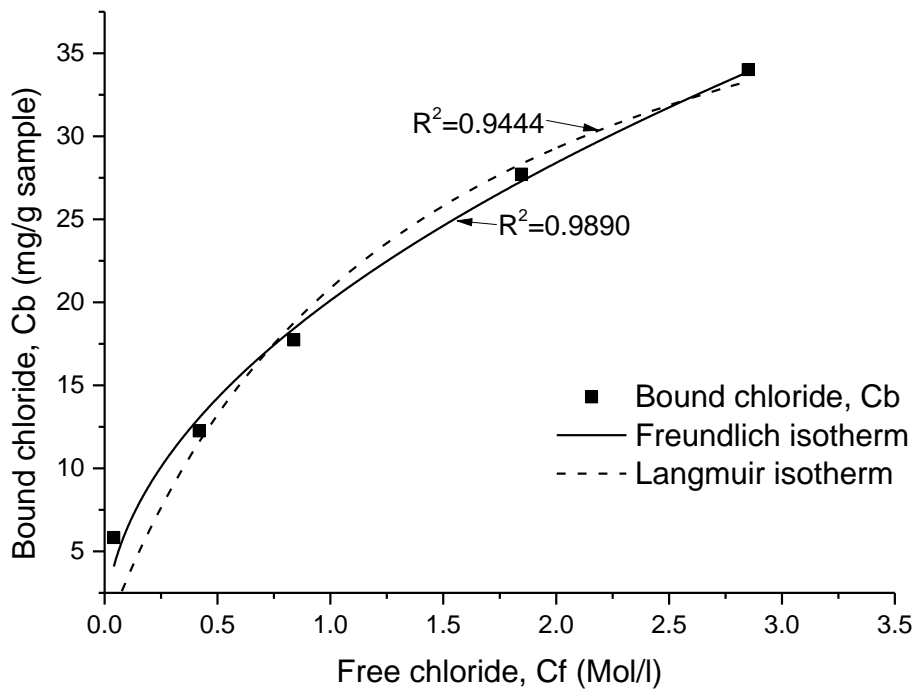
156 W weight of the dry sample in g, which is calculated from the difference in
157 weight of the sample dried in a desiccator at 11%RH and in an oven at
158 105°C.

159 In order to obtain chloride binding isotherms, various concentrations of NaCl solution
160 were used (0.1, 0.5, 1.0, 2.0 and 3.0M). The bound chloride content (C_b) obtained
161 was then plotted against the equilibrium concentration (C_f), after which the chloride
162 binding coefficients (α and β) of the mixes were determined using Freundlich and
163 Langmuir binding isotherms [12] shown respectively in the equations below:

$$C_b = \alpha C_f^\beta \quad (2)$$

$$C_b = \frac{\alpha C_f}{(1 + \beta C_f)} \quad (3)$$

164 Fig. 3 shows the chloride binding coefficients α and β obtained for one of the mixes
 165 using Freundlich and Langmuir binding isotherms. The Freundlich binding isotherm
 166 has been widely used by several researchers [12,26–28], and from the figure, it is
 167 seen that it gives the best fit to the data; hence it was used in determining the
 168 chloride binding coefficients of all the mixes.

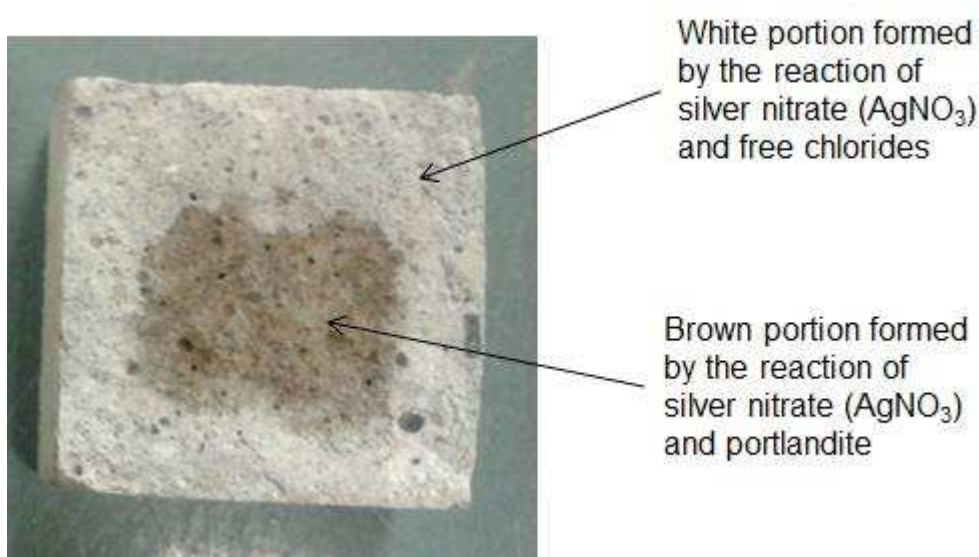


169
 170 **Fig. 3.** Best fit binding isotherm for determining chloride binding coefficients

171 2.3.2 Penetration of free chlorides

172 The depth of free chloride ion penetration was determined using the silver nitrate
 173 (AgNO_3) spray technique. 50 mm mortar cubes were initially cured for 28 days, at
 174 temperatures of 20°C and 38°C. They were then immersed in a 3% NaCl solution
 175 and withdrawn at 14, 28, 56 and 90 days to determine the depths of chloride ion
 176 penetration. The withdrawn samples were split in half and the surfaces of the freshly
 177 split samples were sprayed with a 0.1M AgNO_3 solution. The presence of free

178 chlorides was indicated by the formation of a white precipitate of silver chloride
179 (AgCl), while in the absence of free chlorides the reaction between silver nitrate and
180 portlandite resulted in a brown coloration, due to the formation of silver hydroxide
181 (Fig. 4). By taking linear measurements from the edge of the specimen up to the
182 colour change boundary, the depth of free chloride penetration could be determined.
183 Six to eight measurements were taken per sample. It should be noted that this
184 technique can only indicate the presence of free chloride ion if the concentration is
185 greater than 0.15% by weight of cement [29].



186
187 **Fig. 4.** Colour changes for chloride ingress sample sprayed with 0.1M AgNO_3
188 solution
189

190 2.3.3 Acid soluble or total chloride content

191 40 x 40 x 160 mm mortar samples were cast and cured for 28 days at temperatures
192 of 20°C and 38°C. After curing, about 20 mm thick slice was sawn off from one end
193 of the samples so as to obtain a fresh surface. An epoxy – based paint was used to
194 coat all the sides of the sample except the fresh surface so as to allow for
195 unidirectional chloride ingress. The coated samples were left in the laboratory for 2
196 days to allow for proper curing of the paint, after which they were saturated in

197 deionised water for 24 hours. The saturated samples were then immersed in a tub
198 containing 3% NaCl solution for an exposure/ soaking period of 90 days. The liquid
199 to solid ratio was kept above 12.5 millilitres per square centimetre of exposed
200 surface as recommended in EN 12390:2015 [24], all through the exposure period.

201 At the end of the exposure period, the samples were removed from the tub and
202 wiped dry with a clean cloth. Layers were extracted from the sample by dry cutting.
203 The thickness of the cutting blade was approximately 3 mm. A total of 7 layers (each
204 approximately 5 mm thick) were cut from each sample (See Fig. 5). After cutting,
205 each of the layers was placed in separate polythene bags for grinding. Grinding was
206 done for most of the samples using a mortar and a pestle. The samples were ground
207 such that the particles would pass through a 300 microns sieve. The ground samples
208 were further dried in an oven at 105°C for 24 hours before they were analysed for
209 total chloride content.

210 Total chloride content was determined for each layer using the procedure
211 recommended by RILEM [30]. About 1 gram of the dried samples was weighed and
212 placed in a beaker. 50 ml of concentrated nitric acid (HNO_3) diluted to 1 in 2 parts
213 was added to the sample. After the effervescence had stopped, the solution was
214 heated and allowed to boil for about 1 min. 5 ml of 0.1N silver nitrate solution
215 (AgNO_3) was added to the beaker and the resulting solution was allowed to boil for
216 another 1 min. After this, the solution was allowed to cool down to room temperature
217 and filtered over a filter paper under vacuum. The filter paper and beaker were
218 washed with diluted HNO_3 (diluted to 1 in 100 parts), and collected alongside the
219 filtrate. The final volume of the filtered solution was made up to 200 ml by adding
220 diluted HNO_3 . This was titrated against a 0.05M ammonium thiocyanate solution
221 (NH_4SCN). A blank test was also run using the same procedure outlined above, but

222 without any sample. The total chloride content per mass of the dried sample was
 223 determined using the expression below:

$$\%Cl = \frac{3.5453V_{Ag}M_{Ag}(V_2 - V_1)}{mV_2} \quad (4)$$

224 where:

225 V_{Ag} volume of $AgNO_3$ added in cm^3

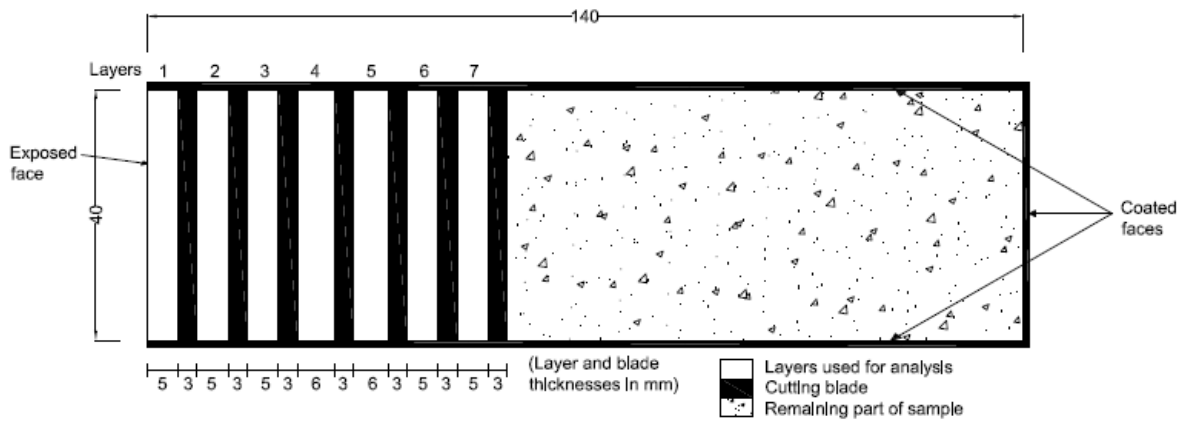
226 M_{Ag} molarity of the $AgNO_3$ solution

227 V_1 volume of NH_4SCN used in the sample in cm^3

228 V_2 volume of NH_4SCN used in the blank test in cm^3

229 m mass of the dried sample used for the test in grams

230 At least three measurements were taken per layer, depending on the amount of
 231 ground sample obtained from the cutting and grinding process. The average total
 232 chloride content obtained per layer was plotted against the distance of the centre of
 233 each layer from the exposed face (fresh surface), to obtain total chloride profiles.



234

235 **Fig. 5.** Schematic showing how layers were extracted from samples after ponding in
 236 3% NaCl solution for 90 days at 20 and 38°C

237 2.3.4 Water soluble chloride content

238 Water soluble chloride content is defined here, as the amount of chloride ion in a
 239 concrete specimen which can be leached out by water at room temperature [31]. It

240 should be noted that this is not the same as the free chloride content, which is taken
241 as the amount of chloride ion dissolved in the pore solution that can be obtained by
242 squeezing concrete samples at high pressures [31].

243 In determining the water soluble chloride content, 5 grams of ground sample was
244 taken from each layer of the samples used for the total chloride content
245 determination test. The ground sample was placed in a plastic bottle. A solid to liquid
246 ratio of 1:20 was used [32], hence 100 ml of distilled water was added to the sample
247 and the plastic bottle was sealed and left to stand for 72 hours at 20°C. At the end of
248 the standing period, the solution was filtered off and the chloride concentration of the
249 filtrate was determined by ion chromatography.

250 The water soluble chloride content, which was taken as the chloride concentration of
251 the filtrate, was expressed in parts per million (ppm) and plotted against the distance
252 of the centre of each layer from the exposed face, to obtain the water soluble
253 chloride profile.

254 2.3.5 SEM-BSE image analysis

255 SEM-BSE image analysis does not provide a detailed 3-dimensional representation
256 of the pore structure, but it can be used to assess the coarse porosity of paste
257 samples [43]. 2 mm thick discs were cut from 28 days old paste samples, which had
258 been cured under saturated lime water at 20°C and 38°C . The samples were
259 hydration stopped using isopropanol, then resin impregnated before polishing. BSE-
260 SEM images were collected for the polished samples using a Carl Zeiss EVO SEM.
261 An accelerating voltage of 15keV was used, combined with a spot size of 500 nm.
262 Electron images were collected at a magnification of x800 and a working distance of
263 8 – 8.5 mm.

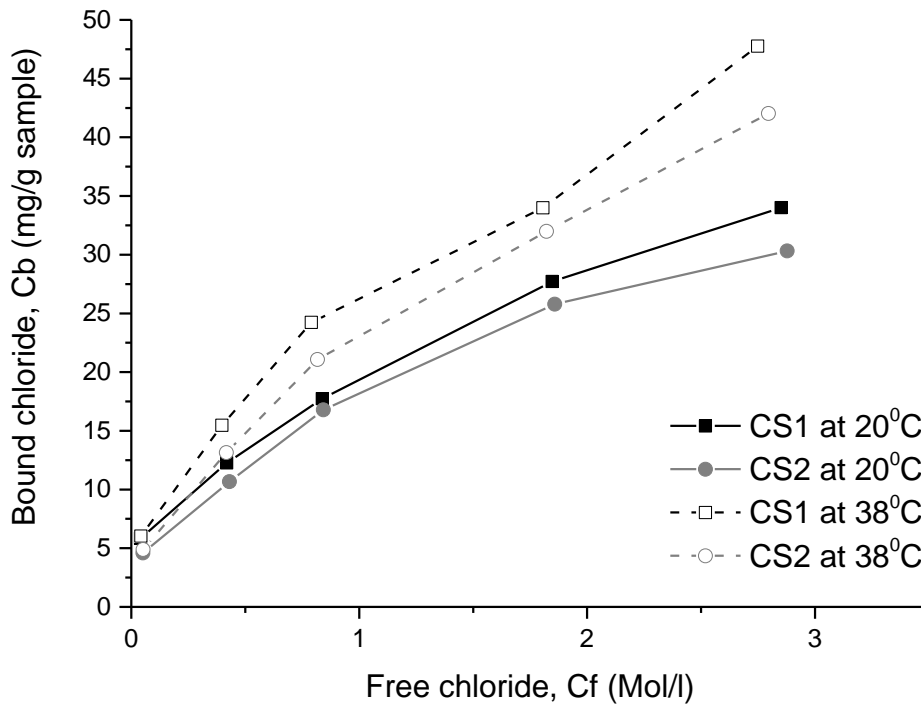
264 This approach enabled differentiation between anhydrous material, hydrated paste
265 and pores. The latter features usually appear as dark spots in the electron images
266 and can be easily distinguished from the hydrated phases by image analysis [33,34].
267 A total of 50 electron images were collected per sample at random and analysed,
268 and the average was taken as the degree of coarse porosity.

269 **3. Results and discussion**

270 3.1 Chloride binding

271 3.1.1 Influence of slag composition

272 Fig. 6 shows the bound chloride content, C_b , obtained from the samples exposed to
273 the different concentrations (C_i) of NaCl solution at 20°C and 38°C. The bound
274 chloride levels were greater for sample CS1 than CS2, and at higher temperatures.
275 There are two explanations for the differences in chloride binding between the two
276 slag blends. Bound chloride in blend CS1, with an overall bulk alumina content of
277 about 7.41%, was consistently higher than that of CS2 (alumina content of 6.08%).
278 Several studies have shown that chloride binding increases with the alumina content
279 [3,10–12] and decreases with the sulphate content [6,11,35] of the cementitious
280 materials. Secondly, it is known that chlorides are also bound on to C-S-H. Previous
281 work has shown that the more basic slag 1 ((C+M)/S = 1.28) hydrated to a greater
282 degree than slag 2 ((C+M)/S = 1.18). As shown in Table 4, after 28 days, about 55%
283 and 62% of slag 1 had hydrated at 20°C and 38°C respectively; while for the slag 2
284 blend, only about 44% and 49% of the slag portion had hydrated [21]. This is
285 supported by the DTG data shown in Fig. 7, where a larger signal attributed to C-S-H
286 was seen in the CS1 blends.



287

288 **Fig. 6.** Chloride binding relationship for the slag blends at 20°C and 38°C

289

290 **Table 4:** Degree of slag hydration at 28 days as determined by SEM image analysis
 291 (taken from [21])

Mix	Temperature	Degree of Hydration (%)	Error
CS1	20°C	54.85	1.00
	38°C	62.40	1.01
CS2	20°C	43.76	1.55
	38°C	48.92	1.50

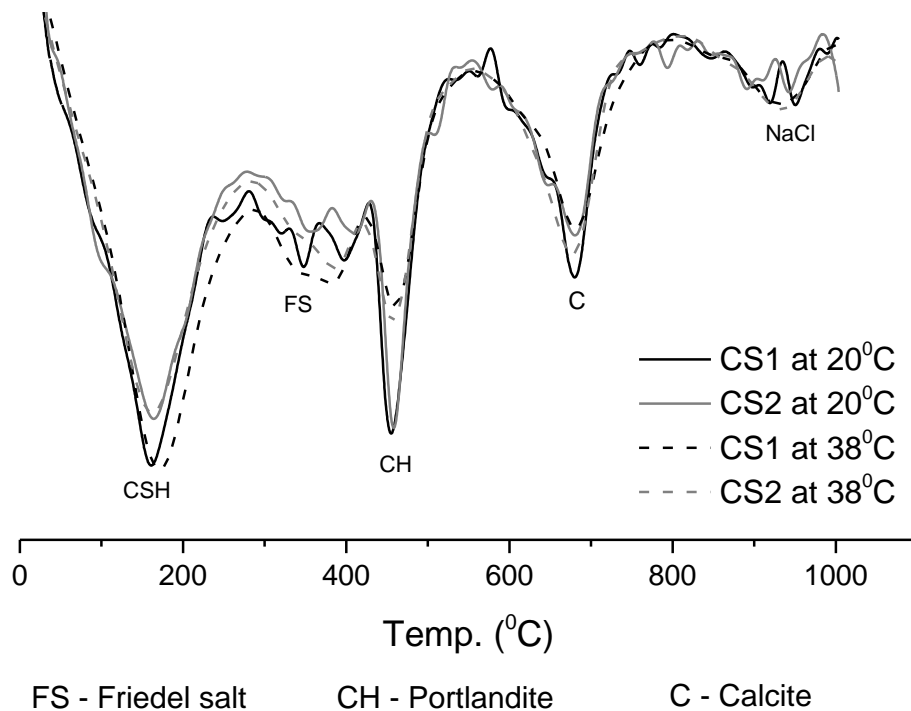
292 3.1.2 Influence of temperature

293 From Fig. 6, at $C_i = 0.1M$, there was no significant difference in the bound chloride
 294 contents obtained at 20°C and 38°C but at C_i of 0.5M and beyond, bound chloride
 295 contents were higher for samples cured and exposed at 38°C. This agrees with
 296 earlier results obtained by Arya et al. [36] in their study of factors influencing chloride
 297 binding in concrete, where they cured OPC paste samples for 4 weeks at
 298 temperatures of 8, 20 and 38°C, and introduced the chlorides into the samples at the

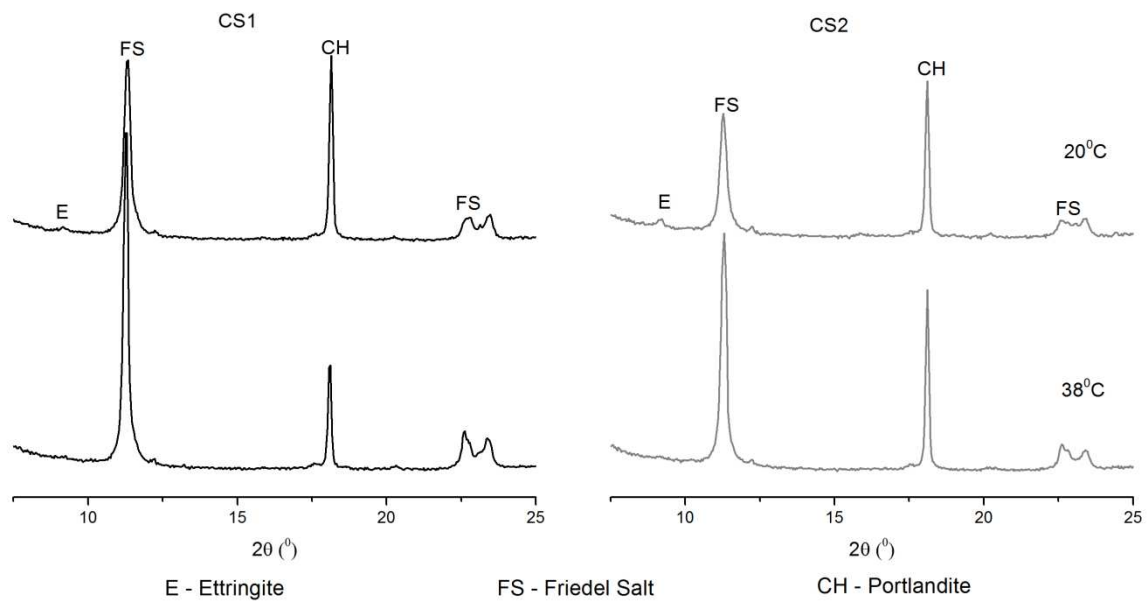
299 point of mixing. They observed that the bound chloride content increased with
300 temperature, and attributed it to faster reaction rates occurring at higher
301 temperatures. Although, the results reported here are for slag blended systems
302 which have been cured for 8 weeks, before testing for binding of external chlorides,
303 the trend is similar. In another study by Zibara [37], an increase in temperature from
304 23°C to 38°C resulted in a decrease in the amount of bound chlorides for host
305 solutions having chloride concentrations between 0.1M and 1.0M, and an increase in
306 the amount of bound chlorides at a concentration of 3.0M. However, the difference at
307 1.0M was minor compared to the increase at 3.0M. Also, it is important to point out
308 that all their test samples were cured at the same temperature of $23 \pm 2^\circ\text{C}$ and
309 tested for chloride binding at temperatures ranging from 7°C to 38°C. In this study ,
310 the samples were cured and tested for chloride binding at temperatures of 20°C and
311 38°C.

312 The increased chloride binding at higher temperatures can be attributed to the higher
313 degree of slag hydration [21]. C-S-H and aluminate phases are principally
314 responsible for chloride binding. These phases are more prevalent at 38°C due to
315 the accelerating effect of temperature on the hydration reaction [38,39]. More so,
316 there is increase in the amount of sulphate ions bound reversibly within the C-S-H
317 phase at higher temperatures, and less calcium sulphate remains available for a
318 reaction with C_3A [40]. Slag hydration is more gradual than that of clinker[41–43],
319 and more greatly affected by temperature [39,44]. Therefore, while clinker hydration
320 would be almost complete after 8 weeks, i.e. the age at which the samples were
321 tested, the degree of slag hydration differed between the samples. Thermal analysis
322 of the samples (Fig. 7) revealed lower portlandite contents in the blends hydrated at
323 38°C. This is due to the consumption of the portlandite by the slags [19,45], thus

324 indicating that the slags had reacted more at 38°C, confirming earlier findings [21].
 325 This can be related to the study by Loser et al. [46], where they showed that chloride
 326 binding was strongly related to the hydration degree of the cement and of the mineral
 327 admixtures. Thermal analysis (Fig. 7) and XRD data (Fig. 8) performed on the
 328 samples at the end of the test show increased signals due to Friedel's salt (FS) for
 329 the samples cured at 38°C, thus confirming the increased chloride binding.



330
 331 **Fig. 7.** DTG plots showing peaks of Friedel's salt (FS) for slag 1 and 2 blend at 20°C
 332 and 38°C for paste samples after immersion in NaCl solution ($C_i = 2.0M$)



333

334 **Fig. 8.** XRD patterns showing peaks of Friedel's salt (FS) for slag 1 and 2 blend at
 335 20°C and 38°C for paste samples after immersion in NaCl solution ($C_i = 2.0M$)

336 3.1.3 Chloride binding isotherms

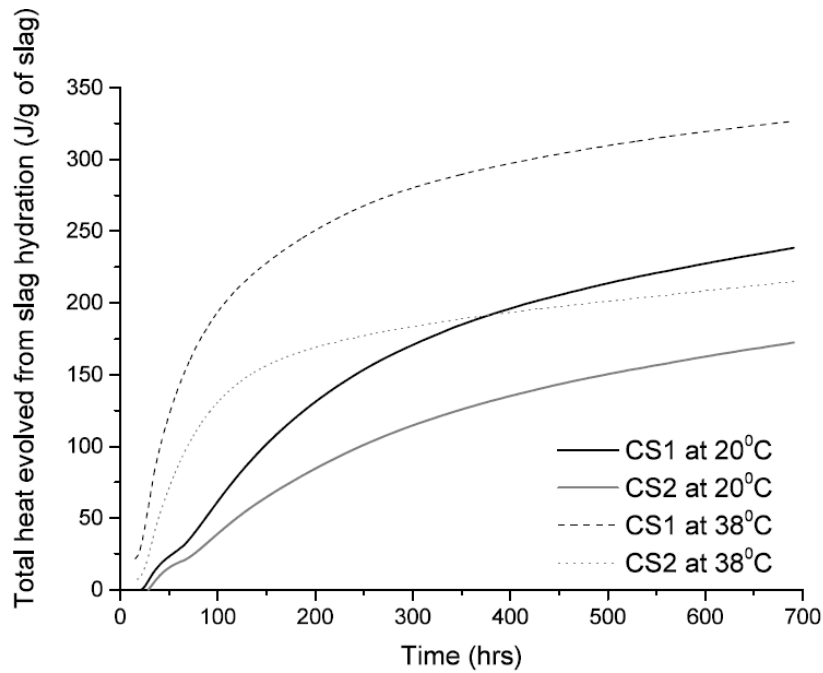
337 The chloride binding coefficients (α and β) obtained by fitting Freundlich's binding
 338 isotherm to the data are shown in Table 5. These coefficients don't have any
 339 physical meaning as they are not material properties, but can be used to give an
 340 indication of the chloride binding capacities of the cementitious materials. The
 341 chloride binding coefficient (α) was greater for the more basic, alumina-rich slag 1
 342 and at higher temperatures. When the temperature was increased from 20°C to
 343 38°C, α increased by about 32% and 27% for CS1 and CS2 respectively. Meanwhile,
 344 α for CS1 was about 11% and 15% higher than that for CS2 at 20°C and 38°C
 345 respectively. The values of α and β shown here are somewhat higher than those
 346 reported by Thomas et al. [12] for similar samples at 23°C. This can be attributed to
 347 the type of samples used. While Thomas et al. [12] used 3 mm thick disc paste
 348 samples, ground samples were used here. Zibara [37] showed that the amount of
 349 chlorides bound by ground samples were higher than that of disc samples.

350 **Table 5:** Chloride binding coefficients obtained using Freundlich's binding isotherm

Mix	Temperature (°C)	α	β	Adj. R ²
CS1	20	20.11	0.50	0.9890
	38	26.46	0.55	0.9839
CS2	20	18.07	0.51	0.9908
	38	23.00	0.58	0.9972

351

352 An interesting observation was that the difference between the chloride binding
353 coefficient (α) of CS1 and CS2 increased as the temperature was raised from 20°C
354 to 38°C (Table 5). This reflects the increase in the degree of hydration (see Table 4),
355 where temperature has a greater effect on the more basic slag 1. Isothermal
356 calorimetry tests conducted on paste samples from the slag blends at 38°C (see Fig.
357 9), indeed confirmed this. Furthermore, referring back to the portlandite contents
358 from Fig. 7, while the levels were similar for both samples at 20°C, the portlan dite
359 content of CS1 was lower than that of CS2 at 38°C, indicating that slag 1 had
360 reacted more.



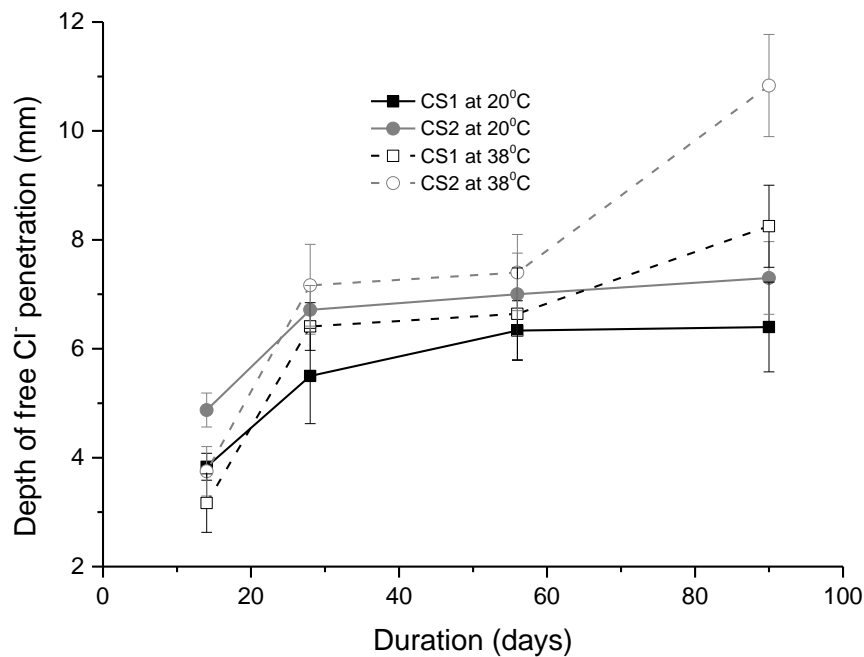
361

362 **Fig. 9:** Slag contribution to total heat evolved as measured by isothermal calorimetry

363 3.2 Chloride diffusion

364 3.2.1 Free chloride penetration

365 The depth of free chloride penetration measured on samples which had been cured
 366 for 28 days before exposure to a 3% NaCl solution is shown in Fig. 10. The
 367 penetration depths were lower for sample CS1 than CS2 at all durations and both
 368 temperatures. After 90 days of exposure at 38°C the depth of penetration of free
 369 chloride ions into CS2 was about 31% higher than that of CS1, compared to a
 370 difference of about 14% at 20°C. This again reflects the degree of slag hydration,
 371 where chlorides are bound (and therefore by definition not free) by hydration
 372 products. This correlates with the results of the chloride binding, where it was seen
 373 that CS1 had a higher chloride binding capacity, and is in agreement with previous
 374 findings by Otieno et al. [13].



375

376 **Fig. 10.** Depth of penetration of free Cl⁻ into mortar samples cured for 28 days before
 377 exposure to a 3% NaCl solution for a period of 90 days.
 378

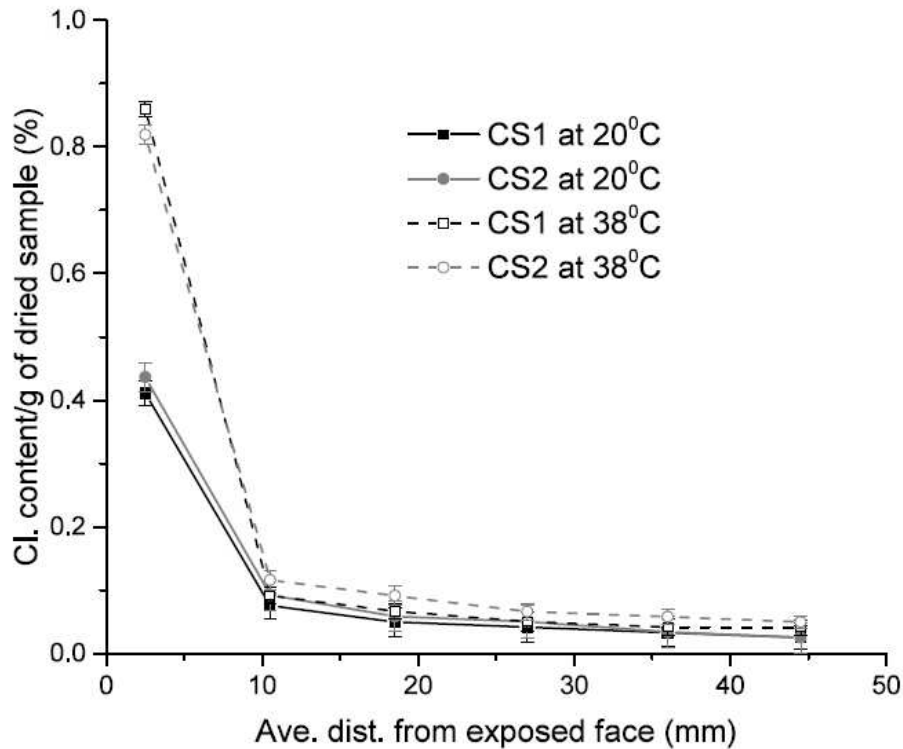
379 As chloride binding was increased at 38°C, this was expected to reflect in the results
 380 of the penetration of free chloride ions (Fig. 10) in that there should be less free
 381 chlorides in the pore solution. This was true for the first 14 days of exposure, as
 382 samples cured and exposed at 38°C had lower chloride penetration depths than
 383 those cured and exposed at 20°C. However, as the samples were exposed for
 384 longer periods, those cured and exposed at the higher temperature showed greater
 385 chloride penetration. Thus, despite the higher chloride binding occurring at 38°C due
 386 to a greater degree of hydration, there was still an increase in the amount of free
 387 chlorides. This is because the porosity at 38°C was much coarser (as seen later in
 388 Section 3.3), allowing greater penetration into the samples. This explains the huge
 389 difference between the chloride penetration depths measured at 20°C and 38°C for
 390 ages beyond 28 days (as seen in Fig. 10), and also agrees with previous studies

391 [47–51] showing that an increase in exposure temperature leads to an increase in
392 the rate of chloride ingress.

393 For the samples cured at 20°C, the depth of chloride penetration did not increase
394 much after 14 days of exposure whereas there was continuous increase at 38°C. A
395 previous study by Goñi et al. [52], where paste samples were cured in demineralised
396 water for 28 days at 20°C before exposing them to NaCl solutions, showed that the
397 ingress of sodium and chloride ions into the paste caused the formation of Friedel's
398 salt in the pores, resulting in a denser microstructure. Other studies [53,54] have
399 shown that curing in chloride environments can influence hydration of the
400 cementitious materials. High temperature curing results in a high initial rate of
401 hydration, retarding subsequent hydration. This produces a non-uniform distribution
402 of hydration products compared with the case of a lower curing temperature [38,55].
403 In this study, the samples exposed at the higher temperature had hydrated to a
404 greater degree, but had a much more open microstructure as evidenced by their
405 coarse porosity (shown later in Section 3.3). However, the samples cured at the
406 lower temperature continued to hydrate in the chloride solution, resulting in the
407 formation of a dense microstructure, thus reducing the rate of chloride ingress into
408 the samples. This might be the reason why the depth of chloride penetration
409 measured for the samples cured at 20°C did not increase much after 14 days of
410 exposure, as compared to at 38°C (Fig. 10).

411 3.2.2 Total and water soluble chloride content

412 Total chloride profiles obtained for samples at the end of the soaking period (90
413 days) are shown in Fig. 11.



414

415 **Fig. 11.** Total chloride profile obtained for mortar samples cured for 28 days before
 416 exposure to a 3% NaCl solution for a period of 90 days.

417

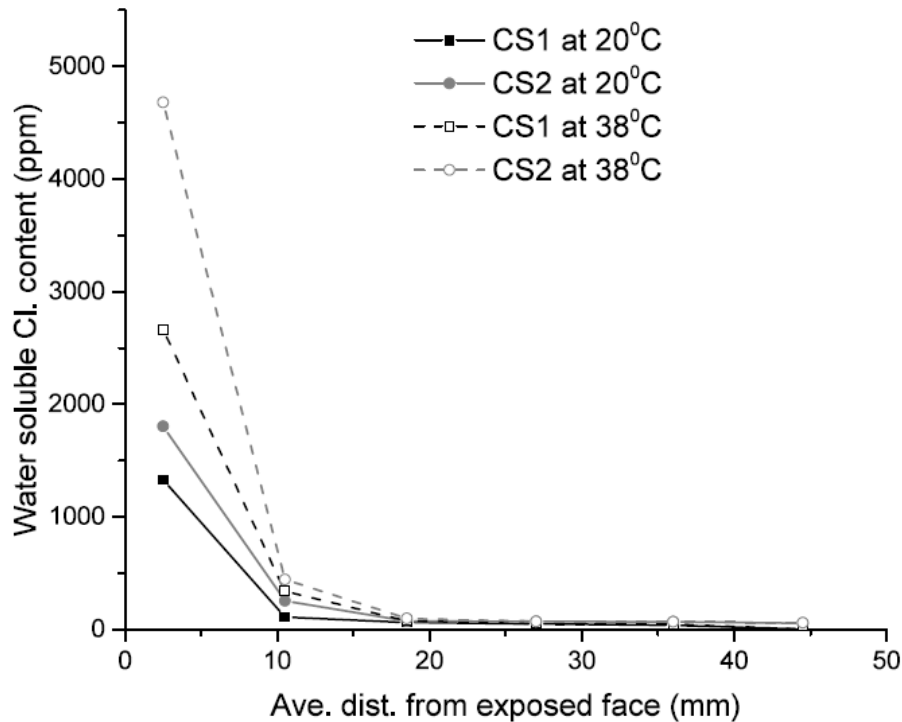
418 The total chloride profiles at 38°C, when compared to those at 20°C are
 419 characterised by very high chloride concentrations at the surface, which decrease to
 420 much lower values within a short distance, and are characteristic of mixes having
 421 high chloride binding capacities [56]. Indeed, the chloride binding results shown in
 422 Fig. 6 showed that there was higher chloride binding at 38°C. This agrees with
 423 results from previous studies [47,49,51,57], and supports the chloride penetration
 424 results (Fig. 10), which showed that there was greater chloride penetration at 38°C.

425 As seen in Fig. 11, the difference in temperature only had a significant effect on the
 426 total chloride content at the region close to the exposed face. At further depths within
 427 the samples, there was no significant difference between the total chloride contents
 428 for the samples cured and exposed at 20°C and 38°C. The reason for this can also
 429 be linked to chloride binding. Since chloride binding was greater at 38°C, this implies

430 that more Friedel's salt was formed. This phase can have a pore blocking effect,
431 slowing down the rate of subsequent chloride ingress [52,58,59].

432 In Fig. 10, CS1 was seen to have lower depths of free chloride penetration than CS2,
433 regardless of temperature. However, Fig. 11 shows only a slight difference between
434 the total chloride contents of CS1 and CS2, with that of CS1 being lower than that of
435 CS2 at both temperatures. The reason for this can be explained from Fig. 12, which
436 shows the water soluble chloride content obtained from the same samples that were
437 used for the total chloride content test.

438 Fig. 12 shows that there was a clear difference in the water soluble chloride contents
439 of CS1 and CS2, especially in the near subsurface region. This supports the results
440 shown in Fig. 10 and can also be linked to chloride binding. While similar amounts of
441 chloride diffused into both slag samples (as seen in Fig. 11), CS1 having a higher
442 chloride binding capacity (see Fig. 6 and Table 5) bound more of the chlorides, thus
443 leading to lower water soluble chloride contents. Fig. 12 also shows that the
444 difference between the water soluble chloride content of CS1 and CS2 is greater at
445 38°C than at 20°C. This also correlates with the chloride binding results shown in
446 Fig. 6 and Table 5, where it was seen that the chloride binding capacity of CS1 was
447 far greater than that of CS2 at 38°C as compared to 20°C, due to the increase in the
448 degree of slag hydration [21].

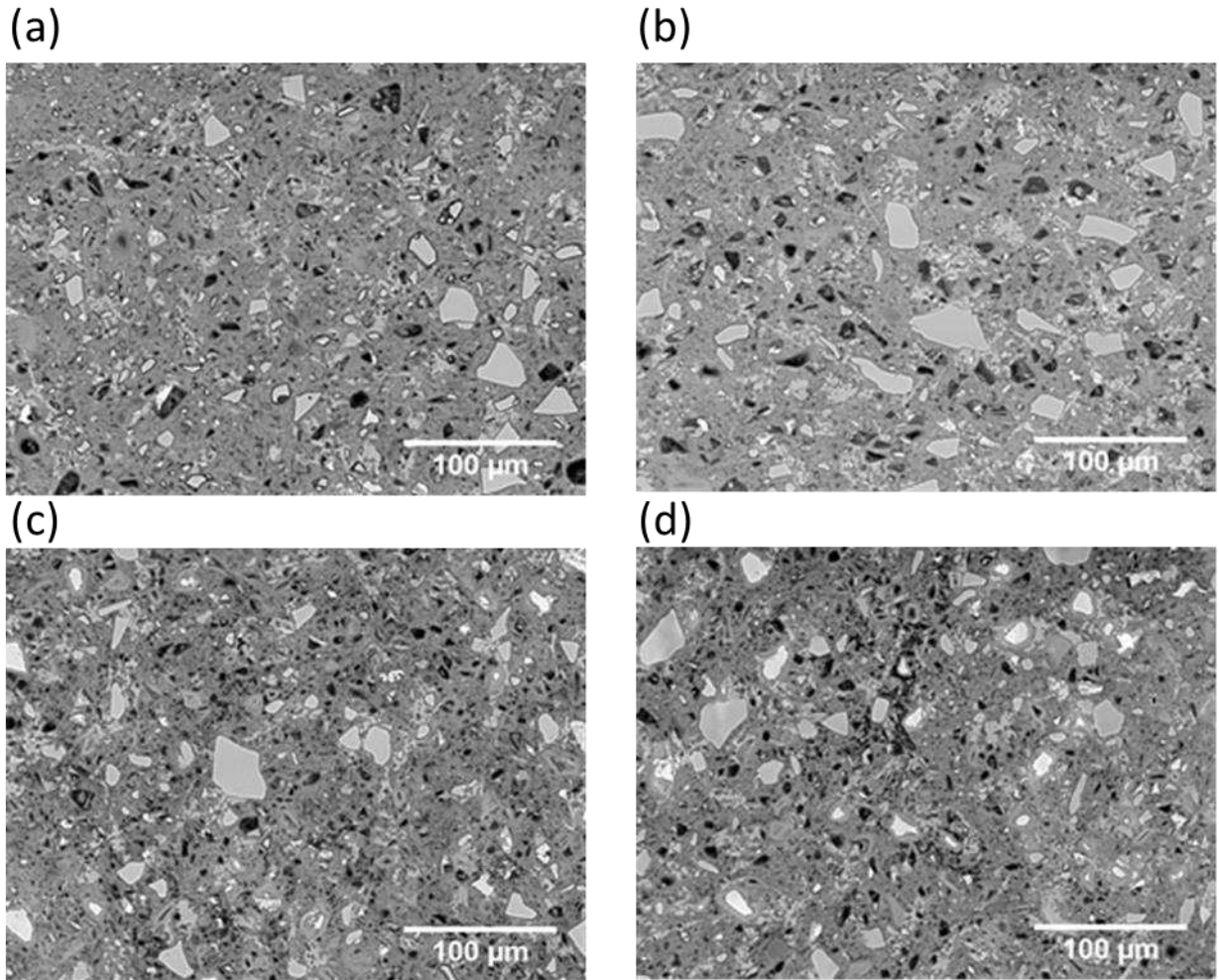


449

450 **Fig. 12:** Water soluble chloride profile obtained for mortar samples cured for 28 days
 451 before exposure to a 3% NaCl solution for a period of 90 days.

452 3.3 Degree of coarse porosity

453 Representative SEM-BSE images of the samples are shown in Fig. 13. The pore
 454 structures of the samples cured at 38°C appeared coarser, consisting of a large
 455 number of clustered pores distributed randomly throughout the sample. Table 6
 456 shows the average coarse porosity measured by grey level imaging from 50 SEM-
 457 BSE images selected at random from paste samples of the two slag blends, cured
 458 for 28 days at temperatures of 20°C and 38°C. Increasing the temperature from 20° C
 459 to 38°C resulted in an increase in the capillary porosity of about 36%. In a nother
 460 study [21], water sorptivity tests conducted on mortar samples prepared from these
 461 same blends showed that the sorptivity coefficient of 28 day old samples increased
 462 by about 90% when curing samples at higher temperature. This explains the
 463 increase in the ingress of chloride ions seen at the high temperature of 38°C, and is
 464 consistent with previous findings [38,60].



465

466 **Fig. 13.** SEM-BSE images of 28 day old samples (a) CS1 at 20°C (b) CS2 at 20°C
 467 (c) CS1 at 38°C (d) CS2 at 38°C. The white coloured features are the anhydrous
 468 cement grains, while the light grey coloured, angular features are the anhydrous slag
 469 grains. The CH and C-S-H phases appear as light and dark grey respectively, while
 470 the dark spots are the capillary pore clusters.

471

472 Comparing the two blends, the coarse porosity of CS1 was only about 7% lower than
 473 that of CS2 at each temperature. This explains the only slight difference in total
 474 chloride contents as seen in Fig. 11. This implies that the diffusion of chlorides into
 475 the slag blends was principally governed by two factors – the chloride binding
 476 capacity of the slag blends and the pore structure, both of which are influenced by
 477 the slags' chemical composition and the curing temperature. Temperature has a
 478 bigger impact than the difference in the chemical composition of the slags.

479

480 **Table 6:** Degree of capillary porosity of paste samples cured for 28 days under
481 saturated lime water at 20°C and 38°C

Mix	Temperature	Coarse porosity (%)	Std. dev.
CS1	20°C	6.5	0.79
	38°C	8.9	0.56
CS2	20°C	7.0	0.47
	38°C	9.5	0.65

482 **4. Summary and Conclusions**

483 This study has shown that chloride binding capacity and the pore structure are
484 two key factors affecting the ingress of chloride ions into slag blended cements.
485 Both of these factors are further influenced by the chemical composition of the
486 slag and the curing temperature. In summary, the following points have been
487 highlighted:

- 488 • The higher chloride binding capacity of the slag 1 blend was a result of its
489 chemical composition. The higher alumina content led to the formation of
490 more Friedel's salt. The greater basicity led to a higher degree of hydration
491 (formation of more C-S-H phases), which resulted in the formation of a finer
492 pore structure and increased chloride binding. These factors, in turn, resulted
493 in lower chloride penetration depths.
- 494 • Curing samples at elevated temperatures (38°C rather than 20°C) resulted in
495 an increase in the degree of slag hydration, which in turn led to an increase in
496 chloride binding. However, the pore structure became coarser, resulting in an
497 increase in chloride ingress.

498 These results should be considered in high temperature environments like
499 tropical marine regions, where concrete structures may be exposed to high
500 temperature conditions and higher concentrations of chloride. Since it is the free

501 chlorides in the concrete that induce corrosion of the embedded steel
502 reinforcement, if SCMs such as slags are to be used in these areas, it is not just
503 sufficient to look at how they influence the rate of chloride diffusion by virtue of
504 their lower porosity, but also on their chloride binding capacities. For such
505 environments, it might be more suitable to use slags of higher basicity and higher
506 alumina content.

507 **Acknowledgements**

508 The authors would like to thank the Petroleum Technology Development Fund
509 (PTDF) of Nigeria for providing the funds for this research.

510 **References**

- 511 [1] X. Shi, N. Xie, K. Fortune, J. Gong, Durability of steel reinforced concrete in
512 chloride environments: An overview, *Constr. Build. Mater.* 30 (2012) 125–138.
- 513 [2] Rasheeduzzafar, S.E. Hussain, S.S. Al-Saadoun, Effect of tricalcium aluminate
514 content of cement on chloride binding and corrosion of reinforcing steel in
515 concrete, *ACI Mater. J.* 89 (1992) 3–12.
- 516 [3] R.K. Dhir, M.A.K. El-Mohr, T.D. Dyer, Chloride binding in GGBS concrete,
517 *Cem. Concr. Res.* 26 (1996) 1767–1773.
- 518 [4] A. Ipavec, T. Vuk, R. Gabrovšek, V. Kaučič, Chloride binding into hydrated
519 blended cements: The influence of limestone and alkalinity, *Cem. Concr. Res.*
520 48 (2013) 74–85. doi:<http://dx.doi.org/10.1016/j.cemconres.2013.02.010>.
- 521 [5] S. Ehtesham Hussain, Rasheeduzzafar, A.S. Al-Gahtani, Influence of sulfates
522 on chloride binding in cements, *Cem. Concr. Res.* 24 (1994) 8–24.
523 doi:[http://dx.doi.org/10.1016/0008-8846\(94\)90078-7](http://dx.doi.org/10.1016/0008-8846(94)90078-7).
- 524 [6] K. De Weerd, D. Orsáková, M.R. Geiker, The impact of sulphate and

- 525 magnesium on chloride binding in Portland cement paste, *Cem. Concr. Res.*
526 65 (2014) 30–40. doi:<http://dx.doi.org/10.1016/j.cemconres.2014.07.007>.
- 527 [7] K. De Weerd, A. Colombo, L. Coppola, H. Justnes, M.R. Geiker, Impact of the
528 associated cation on chloride binding of Portland cement paste, *Cem. Concr.*
529 *Res.* 68 (2015) 196–202.
530 doi:<http://dx.doi.org/10.1016/j.cemconres.2014.01.027>.
- 531 [8] D. Conciatori, F. Laferrière, E. Brühwiler, Comprehensive modeling of chloride
532 ion and water ingress into concrete considering thermal and carbonation state
533 for real climate, *Cem. Concr. Res.* 40 (2010) 109–118.
534 doi:<http://dx.doi.org/10.1016/j.cemconres.2009.08.007>.
- 535 [9] Z. Song, L. Jiang, J. Liu, J. Liu, Influence of cation type on diffusion behavior of
536 chloride ions in concrete, *Constr. Build. Mater.* 99 (2015) 150–158.
537 doi:<http://dx.doi.org/10.1016/j.conbuildmat.2015.09.033>.
- 538 [10] A. Cheng, R. Huang, J.K. Wu, C.H. Chen, Influence of GGBS on durability and
539 corrosion behavior of reinforced concrete, *Mater. Chem. Phys.* 93 (2005) 404–
540 411.
- 541 [11] R. Luo, Y. Cai, C. Wang, X. Huang, Study of chloride binding and diffusion in
542 GGBS concrete, *Cem. Concr. Res.* 33 (2003) 1–7.
- 543 [12] M.D.A. Thomas, R.D. Hooton, A. Scott, H. Zibara, The effect of supplementary
544 cementitious materials on chloride binding in hardened cement paste, *Cem.*
545 *Concr. Res.* 42 (2012) 1–7.
546 doi:<http://dx.doi.org/10.1016/j.cemconres.2011.01.001>.
- 547 [13] M. Otieno, H. Beushausen, M. Alexander, Effect of chemical composition of
548 slag on chloride penetration resistance of concrete, *Cem. Concr. Compos.* 46
549 (2014) 56–64. doi:<http://dx.doi.org/10.1016/j.cemconcomp.2013.11.003>.

- 550 [14] M.V.A. Florea, H.J.H. Brouwers, Modelling of chloride binding related to
551 hydration products in slag-blended cements, *Constr. Build. Mater.* 64 (2014)
552 421–430. doi:10.1016/j.conbuildmat.2014.04.038.
- 553 [15] M. Moranville-Regourd, Cements Made from Blastfurnace Slag, in: *Lea's*
554 *Chem. Cem. Concr.*, 2003: pp. 637–678. doi:10.1016/B978-075066256-
555 7/50023-0.
- 556 [16] M.G. Smolczyk, Effect of the chemistry of the slag on the strengths of blast
557 furnace slags, *Zement-Kalk-Gips*. 6 (1979) 294–296.
- 558 [17] S.C. Pal, A. Mukherjee, S.R. Pathak, Investigation of hydraulic activity of
559 ground granulated blast furnace slag in concrete, *Cem. Concr. Res.* 33 (2003)
560 1481–1486. doi:http://dx.doi.org/10.1016/S0008-8846(03)00062-0.
- 561 [18] D.G. Mantel, Investigation into the hydraulic activity of five granulated blast
562 furnace slags with eight different portland cements., *ACI Mater. J.* 91 (1994)
563 471–477.
- 564 [19] A. Bougara, C. Lynsdale, N.B. Milestone, Reactivity and performance of
565 blastfurnace slags of differing origin, *Cem. Concr. Compos.* 32 (2010) 319–
566 324. doi:http://dx.doi.org/10.1016/j.cemconcomp.2009.12.002.
- 567 [20] ACI-233R-03, Slag Cement in Concrete and Mortar , (2003) 18.
- 568 [21] O.R. Ogirigbo, L. Black, Influence of slag composition and temperature on the
569 hydration and microstructure of slag blended cements, *Constr. Build. Mater.*
570 126 (2016) 496–507. doi:10.1016/j.conbuildmat.2016.09.057.
- 571 [22] EN197-1, Composition, specifications and conformity criteria for common
572 cements, BSI, Brussels, 2011.
- 573 [23] EN196-1, Methods of testing cement, BSI, Brussels, 2005.
- 574 [24] EN12390-11, Determination of the chloride resistance of concrete,

- 575 unidirectional diffusion, BSI, Brussels, 2015.
- 576 [25] T. Luping, L.-O. Nilsson, Chloride binding capacity and binding isotherms of
577 OPC pastes and mortars, *Cem. Concr. Res.* 23 (1993) 247–253.
578 doi:[http://dx.doi.org/10.1016/0008-8846\(93\)90089-R](http://dx.doi.org/10.1016/0008-8846(93)90089-R).
- 579 [26] L. Tang, L.O. Nilsson, A new approach to the determination of pore distribution
580 by penetrating chlorides into concrete, *Cem. Concr. Res.* 25 (1995) 695–701.
581 doi: [http://dx.doi.org/10.1016/0008-8846\(95\)00058-k](http://dx.doi.org/10.1016/0008-8846(95)00058-k).
- 582 [27] O.M. Jensen, M.S.H. Korzen, H.J. Jakobsen, J. Skibsted, Influence of cement
583 constitution and temperature on chloride binding in cement paste, *Adv. Cem.*
584 *Res.* 12 (2000) 57–64. doi: <http://dx.doi.org/10.1680/adcr.2000.12.2.57>.
- 585 [28] D. Panesar, S. Chidiac, Effect of Cold Temperature on the Chloride-Binding
586 Capacity of Cement, *J. Cold Reg. Eng.* 25 (2011) 133–144. doi:
587 [http://dx.doi.org/10.1061/\(ASCE\)CR.1943-5495.0000032](http://dx.doi.org/10.1061/(ASCE)CR.1943-5495.0000032).
- 588 [29] E. Güneyisi, K. Mermerdaş, Comparative study on strength, sorptivity, and
589 chloride ingress characteristics of air-cured and water-cured concretes
590 modified with metakaolin, *Mater. Struct.* 40 (2007) 1161–1171. doi:
591 <http://dx.doi.org/10.1617/s11527-007-9258-5>.
- 592 [30] RILEM, Analysis of total chloride content in concrete, *Mater. Struct.* 35 (2002)
593 583–585. doi: <http://dx.doi.org/10.1007/bf02483128>.
- 594 [31] RILEM, Analysis of water soluble chloride content in concrete, *Mater. Struct.*
595 35 (2002) 586–588. doi: <http://dx.doi.org/10.1007/BF02483129>.
- 596 [32] C. Arya, N.R. Buenfeld, J.B. Newman, Assessment of simple methods of
597 determining the free chloride ion content of cement paste, *Cem. Concr. Res.*
598 17 (1987) 907–918. doi:[http://dx.doi.org/10.1016/0008-8846\(87\)90079-2](http://dx.doi.org/10.1016/0008-8846(87)90079-2).
- 599 [33] K.L. Scrivener, H.H. Patel, P.L. Pratt, L.J. Parrott, Analysis of Phases in

- 600 Cement Paste using Backscattered Electron Images, Methanol Adsorption and
601 Thermogravimetric Analysis, MRS Online Proc. Libr. 85 (1986).
602 doi:<http://dx.doi.org/10.1557/PROC-85-67>.
- 603 [34] K.L. Scrivener, Backscattered electron imaging of cementitious
604 microstructures: understanding and quantification, Cem. Concr. Compos. 26
605 (2004) 935–945. doi:<http://dx.doi.org/10.1016/j.cemconcomp.2004.02.029>.
- 606 [35] Y. Xu, The influence of sulphates on chloride binding and pore solution
607 chemistry, Cem. Concr. Res. 27 (1997) 1841–1850.
608 doi:[http://dx.doi.org/10.1016/S0008-8846\(97\)00196-8](http://dx.doi.org/10.1016/S0008-8846(97)00196-8).
- 609 [36] C. Arya, N.R. Buenfeld, J.B. Newman, Factors influencing chloride-binding in
610 concrete, Cem. Concr. Res. 20 (1990) 291–300.
611 doi:[http://dx.doi.org/10.1016/0008-8846\(90\)90083-A](http://dx.doi.org/10.1016/0008-8846(90)90083-A).
- 612 [37] H. Zibara, Binding of external chlorides by cement pastes, University of
613 Toronto, 2001.
- 614 [38] B. Lothenbach, F. Winnefeld, C. Alder, E. Wieland, P. Lunk, Effect of
615 temperature on the pore solution, microstructure and hydration products of
616 Portland cement pastes, Cem. Concr. Res. 37 (2007) 483–491.
617 doi:<http://dx.doi.org/10.1016/j.cemconres.2006.11.016>.
- 618 [39] J.I. Escalante-García, J.H. Sharp, Effect of temperature on the hydration of the
619 main clinker phases in portland cements: part i, neat cements, Cem. Concr.
620 Res. 28 (1998) 1245–1257. doi:[http://dx.doi.org/10.1016/S0008-8846\(98\)00115-X](http://dx.doi.org/10.1016/S0008-8846(98)00115-X).
- 621
- 622 [40] I. Odler, Hydration, Setting and Hardening of Portland Cement, in: Lea's
623 Chem. Cem. Concr., 2003: pp. 241–297. doi: [http://dx.doi.org/10.1016/B978-](http://dx.doi.org/10.1016/B978-075066256-7/50018-7)
624 [075066256-7/50018-7](http://dx.doi.org/10.1016/B978-075066256-7/50018-7).

- 625 [41] V. Kocaba, E. Gallucci, K.L. Scrivener, Methods for determination of degree of
626 reaction of slag in blended cement pastes, *Cem. Concr. Res.* 42 (2012) 511–
627 525. doi:<http://dx.doi.org/10.1016/j.cemconres.2011.11.010>.
- 628 [42] R. Taylor, I.G. Richardson, R.M.D. Brydson, Composition and microstructure
629 of 20-year-old ordinary Portland cement–ground granulated blast-furnace slag
630 blends containing 0 to 100% slag, *Cem. Concr. Res.* 40 (2010) 971–983.
631 doi:<http://dx.doi.org/10.1016/j.cemconres.2010.02.012>.
- 632 [43] M. Whittaker, M. Zajac, M. Ben Haha, F. Bullerjahn, L. Black, The role of the
633 alumina content of slag, plus the presence of additional sulfate on the
634 hydration and microstructure of Portland cement-slag blends, *Cem. Concr.*
635 *Res.* 66 (2014) 91–101.
636 doi:<http://dx.doi.org/10.1016/j.cemconres.2014.07.018>.
- 637 [44] J.I. Escalante, L.Y. Gómez, K.K. Johal, G. Mendoza, H. Mancha, J. Méndez,
638 Reactivity of blast-furnace slag in Portland cement blends hydrated under
639 different conditions, *Cem. Concr. Res.* 31 (2001) 1403–1409.
640 doi:[http://dx.doi.org/10.1016/S0008-8846\(01\)00587-7](http://dx.doi.org/10.1016/S0008-8846(01)00587-7).
- 641 [45] I. Pane, W. Hansen, Investigation of blended cement hydration by isothermal
642 calorimetry and thermal analysis, *Cem. Concr. Res.* 35 (2005) 1155–1164.
643 doi:<http://dx.doi.org/10.1016/j.cemconres.2004.10.027>.
- 644 [46] R. Loser, B. Lothenbach, A. Leemann, M. Tuchschnid, Chloride resistance of
645 concrete and its binding capacity – Comparison between experimental results
646 and thermodynamic modeling, *Cem. Concr. Compos.* 32 (2010) 34–42.
647 doi:<http://dx.doi.org/10.1016/j.cemconcomp.2009.08.001>.
- 648 [47] B.H. Oh, S.Y. Jang, Effects of material and environmental parameters on
649 chloride penetration profiles in concrete structures, *Cem. Concr. Res.* 37

- 650 (2007) 47–53. doi:<http://dx.doi.org/10.1016/j.cemconres.2006.09.005>.
- 651 [48] A. Lindvall, Chloride ingress data from field and laboratory exposure –
652 Influence of salinity and temperature, *Cem. Concr. Compos.* 29 (2007) 88–93.
653 doi:<http://dx.doi.org/10.1016/j.cemconcomp.2006.08.004>.
- 654 [49] R.J. Detwiler, K.O. Kjellsen, O.E. Gjrv, Resistance to chloride intrusion of
655 concrete cured at different temperatures., *ACI Mater. J.* 88 (1991) 19–24.
- 656 [50] C.L. Page, N.R. Short, A. El Tarras, Diffusion of chloride ions in hardened
657 cement pastes, *Cem. Concr. Res.* 11 (1981) 395–406.
658 doi:[http://dx.doi.org/10.1016/0008-8846\(81\)90111-3](http://dx.doi.org/10.1016/0008-8846(81)90111-3).
- 659 [51] W.A. Al-Khaja, Influence of temperature, cement type and level of concrete
660 consolidation on chloride ingress in conventional and high-strength concretes,
661 *Constr. Build. Mater.* 11 (1997) 9–13. doi:[http://dx.doi.org/10.1016/S0950-](http://dx.doi.org/10.1016/S0950-0618(97)00004-4)
662 [0618\(97\)00004-4](http://dx.doi.org/10.1016/S0950-0618(97)00004-4).
- 663 [52] S. Goi, M. Frias, R. Vigil de la Villa, R. Garca, Sodium chloride effect on
664 durability of ternary blended cement. Microstructural characterization and
665 strength, *Compos. Part B Eng.* 54 (2013) 163–168.
666 doi:<http://dx.doi.org/10.1016/j.compositesb.2013.05.002>.
- 667 [53] H.J. Chen, S.S. Huang, C.W. Tang, M.A. Malek, L.W. Ean, Effect of curing
668 environments on strength, porosity and chloride ingress resistance of blast
669 furnace slag cement concretes: A construction site study, *Constr. Build. Mater.*
670 35 (2012) 1063–1070.
- 671 [54] O.R. Ogirigbo, Influence of slag composition and temperature on the hydration
672 and performance of slag blends in chloride environments, University of Leeds,
673 2016.
- 674 [55] J.J. Brooks, A.F. Al-kaisi, Early strength development of Portland and slag

675 cement concretes cured at elevated temperatures, *ACI Mater. J.* 87 (1990)
676 503–507.

677 [56] L. Tang, Chloride transport in concrete - measurement and prediction.,
678 Chalmers University of Technology, 1996.

679 [57] H.-W. Song, C.-H. Lee, K.Y. Ann, Factors influencing chloride transport in
680 concrete structures exposed to marine environments, *Cem. Concr. Compos.*
681 30 (2008) 113–121. doi:<http://dx.doi.org/10.1016/j.cemconcomp.2007.09.005>.

682 [58] F.P. Glasser, J. Marchand, E. Samson, Durability of concrete — Degradation
683 phenomena involving detrimental chemical reactions, *Cem. Concr. Res.* 38
684 (2008) 226–246. doi:<http://dx.doi.org/10.1016/j.cemconres.2007.09.015>.

685 [59] N.R. Buenfeld, G.K. Glass, A.M. Hassanein, J.-Z. Zhang, Chloride transport in
686 concrete subjected to an electric field., *J. Mater. Civ. Eng.* 10 (1998) 220–228.

687 [60] K.O. Kjellsen, R.J. Detwiler, O.E. GjØrv, Development of microstructures in
688 plain cement pastes hydrated at different temperatures, *Cem. Concr. Res.* 21
689 (1991) 179–189. doi:[http://dx.doi.org/10.1016/0008-8846\(91\)90044-l](http://dx.doi.org/10.1016/0008-8846(91)90044-l).

690